Development and evaluation of a flexible model for CFD simulation of ash deposit formation in biomass fired boilers

Kai Schulze[*,1], Georg Hofmeister[1], Markus Joeller[1,2], Robert Scharler[1,2,3], Ingwald Obernberger[1,2,3], Rob Korbee[4], Mariusz Cieplik[4]

[1] Austrian Bioenergy Centre GmbH, Inffeldgasse 21 B, 8010 Graz, Austria

[2] Institute for Resource Efficient and Sustainable Systems, Graz University of Technology, Inffeldgasse 21B, 8010 Graz, Austria.

[3] BIOS BIOENERGIESYSTEME GmbH, Inffeldgasse 21 B, 8010 Graz, Austria

[4] ECN Energy research Centre of the Netherlands, Unit Biomass, Coal and Environmental Research, Westerduinweg 3, 1755 ZG Petten, The Netherlands

* … Corresponding author
Email: kai.schulze@abc-energy.at; Phone: + 43 316 8739223; Fax: +43 316 8739202

Abstract

Ash deposit formation is one of the major problems in biomass combustion plants. Therefore a flexible CFD (Computational Fluid Dynamics) based model for the prediction of ash deposit formation is being developed which can be applied as a flexible engineering tool for biomass plant design. At the current state of model development, condensation of ash forming vapors as well as deposition of coarse fly ash particles are considered, whereas the sticking probability of silica rich particles is related to the particle viscosity and a reference viscosity.

A first simulation of deposit formation for a pilot-scale combustion plant was in agreement with observations. The results showed that silica rich coarse fly ash particles are the major components of deposit build up. Moreover, the prediction of the fly ash deposition rate is very sensitive to the reference viscosity. Since a broad range of reference viscosities can be found in the literature, which leads to high uncertainties concerning the predicted deposition rates, literature data were used to derive an empirical correlation for the reference viscosity.

Deposit probe measurements using glass particles as synthetic ash were carried out in order to validate the viscosity approach. The comparison of model predictions and experimental results showed significant deviations in capture efficiencies. CFD simulations provided the basis for a detailed investigation and discussion of the observed deviations. Electrical charges of particles, erosion and uncertainties regarding the viscosity approach applied are possible reasons. Therefore, further experimental investigations to support the development of additional sub-models are ongoing in order to improve the prediction accuracy of the deposit formation model.

Keywords: Biomass; CFD modeling; deposit; ash; condensation; particle deposition

1 Introduction

Ash related problems like ash deposit formation have a strong influence on the operation of biomass combustion for the production of heat and electric power, resulting in unscheduled outages and reduced economic efficiencies. Studies have been performed by several researchers (among them Jensen et al., 1997; Baxter et al., 1998; Frandsen et al., 2003) in order to gain more information about the relevant parameters influencing deposit formation in biomass and coal combustion plants.

Since computational power has been increasing continuously, detailed calculations of turbulent reactive flows in combustion plants can be carried out using Computational Fluid Dynamics (CFD), which is a very powerful tool allowing for a spatially and temporally resolved simulation of flow and heat transfer processes. Such simulations for the design and optimization of furnaces and boilers have already been successfully performed e.g. by Kær (2004) and Scharler (2002). However, the CFD based models for the prediction of deposit formation developed by several authors (Kær, 2001; Lee and Lockwood, 1999; Mueller et al., 2003) are limited to a small amount of ash forming compounds or to a single mechanism. Modeling of ash deposit formation is still a challenge due to its high complexity and, therefore, a flexible CFD model taking fuel and plant operation into account has yet to be developed.

Detailed descriptions of ash chemistry as well as relevant transport and deposit formation mechanisms are necessary to describe ash deposit formation in biomass fired boilers. Therefore a new CFD based ash deposit

formation model is being developed. At the present stage of model development, the time-dependent deposit growth and its influence on heat transfer in the furnace and in the radiative section of the boiler considering the condensation of ash forming vapors and the deposition of silica rich coarse fly ash particles can be described. The sticking probability of silica rich particles is related to the particle viscosity and a reference viscosity. The mechanisms of erosion as well as aerosols formation/precipitation are not considered in the deposit formation model at the moment.

First simulations of deposit formation in the furnace and in the radiative section of the fire tube boiler of a pilot-scale grate furnace equipped with a fire tube boiler (440 kW_{th} nominal boiler load) could be confirmed by observations (see also Forstner et al., 2006; Scharler et al., 2004). Additionally, a sensitivity analysis concerning the influence of the deposit formation model parameters on the simulation results was performed within the scope of this work. The results showed that the deposition of coarse fly ash particles is a dominant effect in deposit formation. In addition, it was found that the prediction of the ash deposition rate is very sensitive to the reference viscosity of the viscosity approach applied as stickiness model for silica rich particles. Since a broad range of reference viscosities can be found in the literature, which leads to high uncertainties concerning the predicted deposition rates, literature data were used to derive an empirical correlation for the reference viscosity as a function of the kinetic energy of the particles. Moreover, additional experimental investigations with a deposit probe in a lab-scale combustion simulator and glass particles as synthetic ashes were performed by ECN. These experiments should expand the reference viscosity data base and serve as a basis for the validation of the viscosity approach using the empirically derived function. The comparison of model predictions and experimental results showed significant deviations of the particle capture efficiencies. CFD simulations performed in order to investigate flow and temperature influences provided the basis for a detailed investigation and discussion of the observed deviations as well as of the stickiness approach applied.

2 Modeling

The simulation of the ash deposit formation in the furnace and the boiler is performed in a post-processing mode based on the results of the preceding CFD combustion simulation (for an overview about the overall CFD model for deposit formation including the combustion simulation procedure see section 2.1). The CFD simulation domain comprises the combustion above the fuel bed on the grate up to the exit of the radiative boiler section. The simulation of deposit formation on the surfaces of the convective heat exchanger tube bundles is not possible at the present stage of model development. Since simulation results showed, that deposit formation is dominated by coarse fly ash particles (see chapter 0) the viscosity approach as stickiness model and especially the reference viscosity as highly sensitive modeling parameter are discussed in detail in section 2.2 of this chapter.

2.1 Modeling of deposit formation

The simulation of solid biomass combustion on the grate and the release of flue gas components from the fuel bed is performed using an empirical biomass fuel model which is based on experimental data (Scharler, 2001). Profiles of velocity, temperature and composition of the released flue gas are calculated in order to provide the boundary conditions for the subsequent simulation of turbulent reactive flow in the combustion chamber. Additionally, the empirical model was extended in order to determine the release of coarse fly ash particles (classified in different chemical classes and particle sizes) and ash forming vapors (KCl, $(KCl)_2$, K_2SO_4, K_2CO_3, NaCl, $(NaCl)_2$, Na_2SO_4, Na_2CO_3, PbO, $PbCl_2$, ZnO, and $ZnCl_2$), based on ash balances performed over the combustion plant.

The simulation of turbulent reactive flow in furnace and boiler (CFD combustion simulation) is performed using the Realizable k-ε model for turbulence, the Discrete Ordinate Model for radiation and the Eddy Dissipation Model in combination with a global methane 3-step reaction mechanism including the flue gas components CH_4, CO, CO_2, H_2, H_2O and O_2 for gas phase combustion.

The simulation of deposit formation is performed in a post-processing step based on the preceding simulation of the turbulent reactive flow in the furnace and boiler. Two mechanisms are presently considered in modeling ash deposition on the furnace and boiler walls: condensation of ash forming vapors and precipitation of coarse fly ash particles. A third mechanism, the formation and deposition of aerosols, has not yet been implemented in the deposit formation model. The ash forming vapors are released from the fuel bed and are transported through the combustion plant using the continuum approach (Euler approach). In order to reduce the number of transport equations, the ash forming vapors are split up into their chemical elements (C, Cl, K, Na, O, Pb, S, Zn). The local concentrations of ash forming vapors in the computational cells are determined using thermodynamic equilibrium calculations (except kinetically limited formation of sulfates like Na_2SO_4 or K_2SO_4 which are considered by a separate approach (Forstner et al., 2006) in combination with an In-Situ Adaptive Tabulation algorithm (ISAT) in order to reduce computation time considerably. The thermodynamic equilibrium

calculations are carried out using the software Chemapp with the standard FactSage database. The condensation of ash forming vapors is modeled based on a mass transfer approach (Baehr and Stephan, 1996):

$$\dot{N}_{cond} = \beta \cdot (c_\infty - c_w), \qquad \textbf{Equation 1}$$

where $\dot{N}_{cond}$ is the condensation flux per area, β is the mass transfer coefficient, c_∞ is the free stream concentration and c_w the saturation concentration on the wall. In order to simulate the deposition of coarse fly ash particles, a representative number of particles is released from the fuel bed and transported through the combustion plant using the Lagrangian approach. Turbulent effects on the particle trajectories are modeled using a stochastic tracking method (Discrete Random Walk Model). In the event of particle impaction the particle either sticks to the wall or rebounds. According to Walsh et al. (1990), the total sticking probability of an impacting particle p_{tot} is a function of the sticking probability of the particle p_{part} itself and the sticking probability of the wall p_{wall}:

$$p_{tot} = p_{wall} \cdot p_{part} + p_{wall} \cdot (1 - p_{part}) + (1 - p_{wall}) \cdot p_{part}\,. \qquad \textbf{Equation 2}$$

According to the different sticking behavior of silica rich and salt rich particles different modeling approaches have to be considered. In this work, however, only silica rich coarse fly ash particles were treated. The sticking probability p_{part} of these particles is calculated by the relation of the particle viscosity μ_{part} and the reference viscosity μ_{ref} (see chapter 2.2). The sticking probability of the condensed deposit layer p_{cond} is determined by an approach of Backman et al. (1997) which was been derived for salts. This approach assumes that the condensed deposit layer is not sticky if the melt fraction is smaller than 0.15. The sticking probability rises linearly from 0 to 1 for melt fractions between 0.15 and 0.7 and equals 1 for melt fractions greater than 0.7. Moreover, the melt fraction of the layer is calculated by using thermodynamic equilibrium calculations. Since the deposit layer on the wall is a mixture of coarse fly ash particles and condensed vapors, the total sticking probability of the wall p_{wall} is calculated by mass weighting of the stickiness of the deposited particles p_{part} and the condensed vapors p_{cond}. Furthermore, the effects of erosion due to impacting particles or shear stresses of the flue gas have not been considered in the deposit formation model yet, although they have a influence on deposit build up. However, the effects of erosion are the subject of further investigations and will be modeled in future. Finally, the time dependent deposit build up is taken into account by a quasi-stationary time step calculation, where the change of the heat transfer coefficient of the deposit layer is calculated according to Richards et al. (1993). Since the time dependent deposit build up is affected by erosion, which is not yet implemented in the deposit formation model, only short term deposit build up is investigated within this work.

2.2 Viscosity based stickiness model for silica rich fly ash particles

The calculation of the sticking probability p_{part} of a silica rich particle is based on the assumption of Walsh et al. (1990), where p_{part} is a function of the particle viscosity μ_{part} and a reference viscosity μ_{ref} (Equation 3):

$$p_{part} = \frac{\mu_{ref}}{\mu_{part}} \qquad \mu_{part} > \mu_{ref}\,,$$
$$p_{part} = 1 \qquad \mu_{part} \le \mu_{ref}\,. \qquad \textbf{Equation 3}$$

The reference viscosity μ_{ref} indicates the maximum viscosity of a particle with which the particle has a 100% probability of sticking. The particle viscosity μ_{part} is determined using the viscosity model of Urbain et al. (1981) or Senior et al. (1995) (depending on the chemical composition of the particles).

The values for the reference viscosities μ_{ref} found in the literature are constant values varying from 8 Pa s [Walsh et al. (1990)] to 10^6 Pa s [Richter (2003)]. This large range of reference viscosities has a significant influence on the calculated sticking probability and, following, on the deposited mass. Therefore, in order to achieve a better understanding of the sticking criterion defined in Equation 3 and to find reasonable values for the reference viscosities, experimental investigations were performed by Srinivasachar et al. (1990) and Richter (2003). The authors used synthetic silica rich ashes (glass particles) and studied the sticking behavior on ceramic deposit probes. In both cases the chemical compositions of the glass particles were similar (see Table 1). The measurements were performed with varying gas velocities, particle diameters and gas temperatures.

Table 1: Chemical compositions of glass particles used in experimental deposit probe measurements (source: Richter, 2003; Srinivasachar et al., 1990)

source		SiO_2	Al_2O_3	FeO	CaO	MgO	Na_2O	K_2O	TiO
Richter	[wt%]	72.9	0.8	0.18	9.3	3.6	12.9	0.2	0.1
Srinivasac	[wt%]	72.0	-	-	8.0	5.0	15.0	-	-

The results of Srinivasachar et al. (1990) and Richter (2003) (see Figure 1) are provided in the form of measured particle capture efficiencies on the probes and calculated particle viscosities as a function of particle temperatures at constant particle velocities. Additionally, Richter (2003) showed a relation between reference viscosities μ_{ref} and relative kinetic energy of the impacting particles. The relation is shown in Figure 2, where kinetic energies are normalized with the kinetic energy of the smallest particle ($E_{kin,0}$ = 4.35e-11 J) studied in the work of Srinivasachar et al. (1990). The diagram with logarithmic coordinates shows a linear relation between $\log_{10}(\mu_{ref})$ and $\log_{10}(E_{kin}/ E_{kin,0})$, which can be written as:

$$\log_{10}\left(\mu_{ref}\right) = -0.9699 \cdot \log_{10}\left(\frac{E_{kin}}{E_{kin,0}}\right) + 5.5962 \,. \qquad \textbf{Equation 4}$$

The reference viscosity μ_{ref} as function of E_{kin} which is given in Equation 4, is related to the averaged free stream velocity of all particles before approaching the deposit probe. Consequently, the effective particle impaction velocity and angle are not considered. Presently, it is assumed that the calculated reference viscosity μ_{ref} is also applicable to individual particles, although the relation for μ_{ref} was globally derived for all impacting particles. It is also assumed that the chemical composition of the material does not influence μ_{ref}. This assumption cannot be verified since the chemical compositions of the glass particles used by Srinivasachar et al. (1990) and Richter (2003) are very similar.

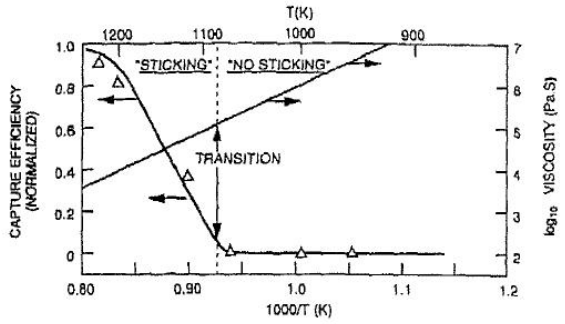

Figure 1: Measured capture efficiencies and calculated viscosity as a function of temperature of glass particles (53µm < d_p < 74 µm) at a velocity of 4 m/s (source: Srinivasachar et al., 1990)

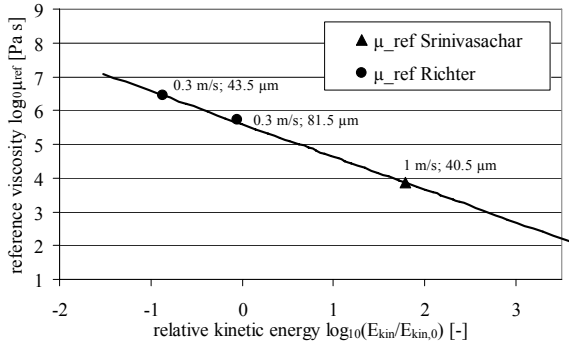

Figure 2: Measured reference viscosities μ_{ref} as a function of relative kinetic energy of impacting particles (E_{kin}…kinetic energy, $E_{kin,0}$…kinetic energy of reference particle source: Srinivasachar et al., 1990; Richter, 2003)

Since data from the literature are only available for adiabatic deposit probes and not within the range considered for biomass combustion plants (see section 0), additional experiments were carried out by ECN with a cooled deposit probe. These measurements should expand the reference viscosity data base and serve as a basis for the validation of the viscosity approach including the empirically derived reference viscosity function.

3 Test and analysis of the CFD deposit formation model for a pilot-scale combustion plant

In order to verify the deposit formation model and to investigate the relevant modeling parameters, simulations for a Low-NO_x pilot-scale biomass grate furnace including air and flue gas recirculation staging as well as with a subsequent fire tube boiler were performed (440 kW_{th} nominal boiler load, see Figure 3). As already mentioned, the simulation domain comprises the furnace from above the fuel bed and the exit of the radiative fire tube. Operation data from test runs with waste wood as fuel was taken as a basis for the boundary conditions of the CFD simulation (see Figure 3).

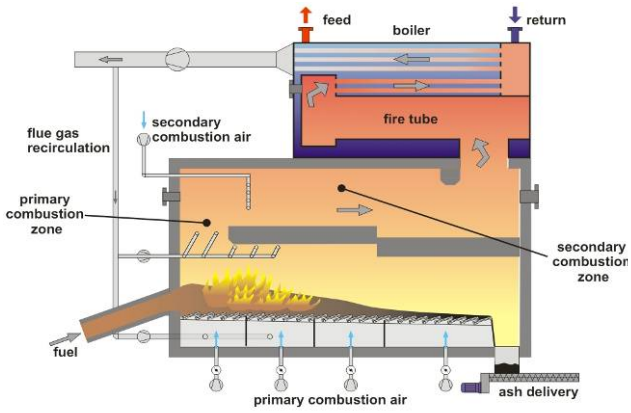

parameter	value	unit
fuel	waste wood	
boiler load	391	[kW_{th}]
fuel flow rate	143	[kg/h w.b.]
moisture content	34.7	[wt%]
ash content	2.7	[wt% d.b.]
total air ratio	1.84	[-]
flue gas recirculation ratio	0.22	[-]
adiabatic flame temperature	937	[°C]
averaged cooling water temperature	72	[°C]

Figure 3: Scheme of the biomass combustion plant and operating parameters. The CFD simulation domain of combustion and ash deposition includes the furnace and the radiative section (fire tube) of the boiler. (w.b.: wet base; d.b.: dry base)

In order to determine total mass flows of ash forming elements released from the fuel bed, a mass balance over the combustion plant was performed for the test run period. It was assumed that the amount of ash that does not end up in the bottom ash is released to the gas phase or entrained as fly ash. The gaseous fraction of ash released was calculated with release factors for the single elements determined by the element balances performed (Table 2). These release factors define the ratio of single element mass fluxes in the gas phase to the total mass fluxes introduced with the fuel. The mass flow of gaseous elements released amounts to 0.107 kg/h. The mass flow of entrained silica rich particles is 0.872 kg/h.

Table 2: Element concentrations in the flue gas of ash forming elements released from the fuel bed as well as gaseous and solid element fractions

element	fraction of fuel flow rate (d.b.) [wt%]	fraction gaseous [%]	fraction solid [%]
Al	0.55e-3	-	100%
Ca	4.71e-3	-	100%
Cl	0.57e-3	100%	-
Fe	0.52e-3	-	100%
K	0.88e-3	16%	84%
Mg	0.84e-3	-	100%
Na	0.44e-3	9%	91%
Pb	0.10e-3	100%	-
S	0.53e-3	30%	70%
Si	1.98e-3	-	100%
Zn	0.16e-3	90%	10%

In order to classify the coarse fly ash particles entrained from the packed bed with respect to chemical compositions and size distributions, a SEM/EDX (Scanning Electron Microscopy / Energy Dispersive X-Ray spectrometry) analysis of the furnace fly ash was performed for 5 particle size classes (d_p < 40µm, 40-80µm, 80-160µm, 160-400µm and 400-800µm). For the chemical classification, particles with similar chemical compositions were associated to specific chemical classes. Since the deposit formation model does not cover the stickiness of salt rich particles at the moment, the classified particles were divided into silica rich and salt rich particles. The results for the classification of released silica rich particles are shown in Table 3.

Firstly, the simulations of deposit formation in the plant with the new correlation for reference viscosities (see section 2.2) were performed. Moreover, it was assumed that the walls were clean at the considered start of plant operation. The simulation results showed a different deposit formation behavior in the furnace and in the water cooled fire tube.

The deposit build up in the primary and secondary combustion zone of the furnace is dominated by coarse fly ash particles (Figure 5). High deposition rates were obtained especially around the nozzles for the injection of secondary air and recirculated flue gas as well as in the flow redirection zone between the primary and secondary combustion zone. In these regions the coarse fly ash particles cannot follow the gas flow due to inertia forces and hit the wall, which leads to a high impaction rate there. The high flue gas temperature which lies between 1,000°C and 1,350°C in this section results in low particle viscosities and thus high sticking probabilities.

Table 3: Entrained coarse fly ash particles (silica rich), classified according to chemical composition and size distribution

chemical class \ mean diameter [µm]	20	60	120	280	600	mass flow [kg/h]
$0.3AlO_3$-2CaO-MgO-$2SiO_2$	0%	9%	49%	34%	8%	0.052
Al_2O_3-2CaO-Na_2O-$4SiO_2$	4%	16%	26%	41%	13%	0.238
$0.2Al_2O_3$-CaO-$2SiO_2$	1%	15%	28%	41%	16%	0.144
3CaO-MgO-$2SiO_2$	8%	36%	21%	34%	1%	0.104
3CaO-$2SiO_2$	6%	26%	22%	42%	4%	0.153
CaO-$6SiO_2$	0%	0%	0%	59%	41%	0.020
K_2O-$4SiO_2$	0%	2%	21%	57%	19%	0.102
SiO_2	1%	0%	6%	79%	14%	0.059
						0.872

In the water cooled fire tube, deposit formation by coarse fly ash particles decreases due to lower particle temperatures and thus lower sticking probabilities but is still of importance due to high local ash particle impaction rates of the ash particles. Condensation of ash forming vapors occurs mainly in the fire tube (Figure 4) due to the fact that the wall temperature of the fire tube is very low compared to that of the furnace walls. The maximum condensation mass flux is observed above the inlet of the fire tube and in the middle section of the turning chamber between the fire tube and the first convective boiler duct. At these sections the flue gas velocity is high, resulting in a high heat and mass transfer coefficient respectively a high condensation rate. In contradiction to the furnace, both effects, coarse fly ash deposition and condensation of ash vapors, are of the same importance in the boiler. However, the deposition rates in the boiler are mostly smaller than in the furnace (see Figure 7).

In general, simulation results showed that the impaction of coarse fly ash particles dominates the deposit formation in the combustion plant, particularly in the furnace. Therefore the viscosity approach applied as stickiness model for silica rich particles was investigated in greater detail.

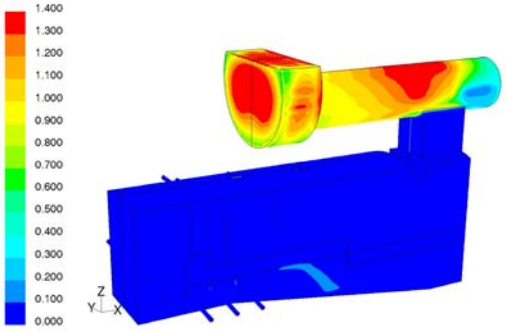

Figure 4: Total condensation mass flux of ash forming vapors considered on furnace and fire tube boiler walls in mg/(m^2s)

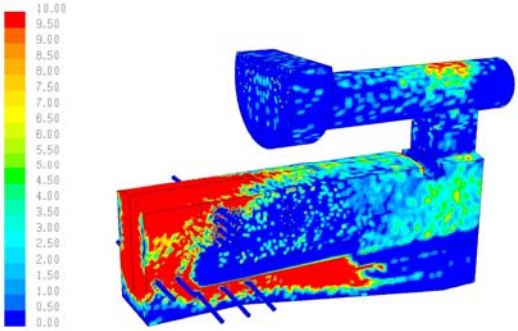

Figure 5: Coarse fly ash particle mass flux (deposited particle mass) to furnace and fire tube boiler walls in mg/m^2s. (Calculation of reference viscosity according to Equation 4)

Since there is a broad variation of literature data on reference viscosity (10 Pa s < μ_{ref} < 10^6 Pa s) a parameter study concerning the influence on the deposit formation behavior was performed based on these data. The results of this parameter study are illustrated in Figure 6, where the fraction of total deposited particle mass related to the total particle mass released from the fuel bed is plotted as a function of the reference viscosity μ_{ref}. Figure 6 shows that the deposited mass is highly dependent on the reference viscosity μ_{ref}. For $\mu_{ref} > 10^6$ Pa s almost all impacting particles that contact the wall stick on the wall, since the viscosity of particles μ_{part} is lower than 10^6 Pa s due to the high temperatures in furnace and fire tube. Only particles of chemical classes SiO_2 and 3CaO-$2SiO_2$ do not precipitate because of their high viscosity levels. Figure 6 shows that the difference between the calculated total deposited masses by using the proposed reference viscosities of Walsh et al. (1990) (8 Pa s) and Richter (2003) ($10^{6.44}$ Pa s) is approximately 100%. This large difference indicates a very high sensitivity of the quantitative prediction of deposit build up by coarse fly ash particles on the reference viscosity μ_{ref}.

As already mentioned, the broad range of reference viscosities found in the literature leads to high uncertainties concerning the predicted deposition rates. Therefore, literature data were used to derive an empirical correlation for the reference viscosity as a function of the kinetic energy of the particles (see chapter 2.2). Figure 7 illustrates the distribution of reference viscosities μ_{ref} in the pilot-scale plant for all impacting particles, with μ_{ref} being

calculated as a function of particle kinetic energies (Equation 4). According to this figure, about 70% of the calculated particle reference viscosities μ_{ref} lie between 30 Pa s and 10^4 Pa s.

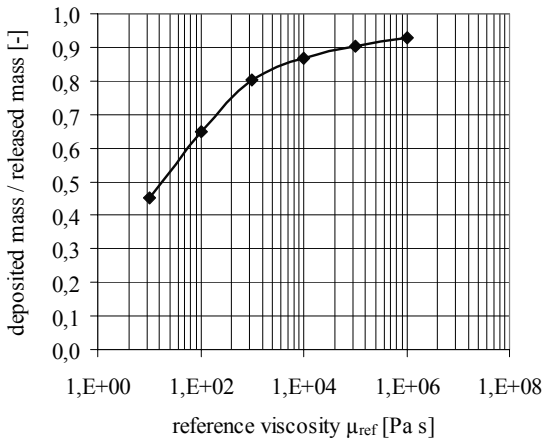

Figure 6: Fraction of deposited mass by coarse fly ash particles in the furnace and fire tube as a function of reference viscosities μ_{ref} (constant values)

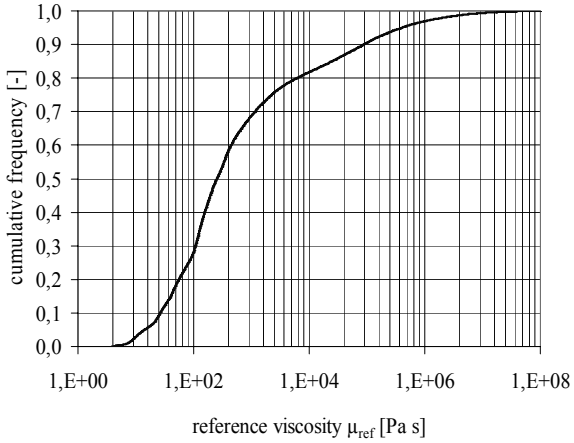

Figure 7: Distribution of μ_{ref} in the pilot-scale plant for all impacting particles (μ_{ref} is a function of kinetic energy, Equation 4). Fraction of deposited mass in the plant is 0.78 (compare Figure 6)

Although it was shown that the determination of μ_{ref} has a significant influence on the quantitative prediction of deposit build up, the reference viscosity had no significant influence on the qualitative prediction of local deposit formation (see Figure 8: reference viscosity 10 Pas and Figure 9: reference viscosity 10^6 Pa s). The comparison of both figures showed that the simulated distribution of deposited ash is very similar, only the amount of deposited mass changes. This qualitative agreement can be explained by the variation of chemical particle classes, which have different viscosities as a function of temperature and therefore a different sticking probability with respect to the reference viscosity. Consequently the numbers of precipitated particle classes increases with rising reference viscosities, whereas the spatial precipitation does not change.

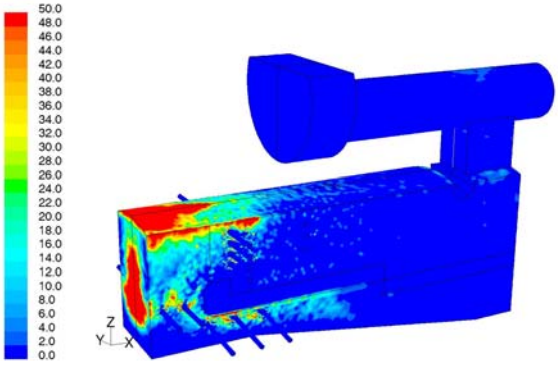

Figure 8: Coarse fly ash particle mass flux (deposited particle mass) to furnace and boiler walls in mg/m^{2}s (μ_{ref} = 10 Pa s)

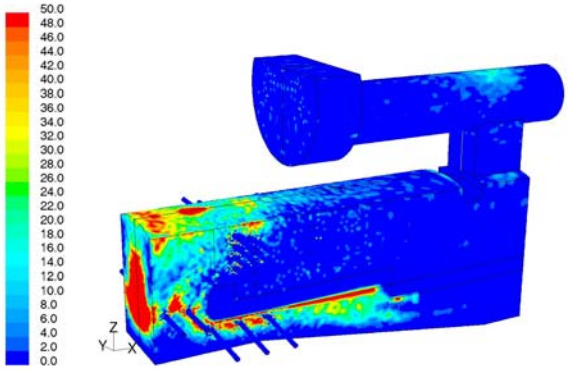

Figure 9: Coarse fly ash particle mass flux (deposited particle mass) to furnace and boiler walls in mg/m^{2}s (μ_{ref} = 10^6 Pa s)

Since the measured reference viscosities found in literature do not cover the range of reference viscosities calculated for the pilot-scale plant (compare Figure 2 and Figure 7), additional lab-scale experiments were performed in order to validate the viscosity approach including the reference viscosity in the typical range of a biomass combustion plant.

4 Investigations of particle stickiness behavior

As already mentioned in the previous chapter, Srinivasachar et al. (1990) and Richter (2003) performed deposit probe measurements using “synthetic” ashes (glass particles) in order to get a better understanding of the stickiness behavior of viscous and silica rich particles. However, only three reference viscosity values could be derived using the data of these authors. Therefore, additional deposit probe measurements were performed by

ECN Biomass, Coal and Environmental Research to expand the data base and to validate the viscosity approach as a stickiness model for silica rich particles including the derived reference viscosity correlation for the operating conditions of biomass combustion plants (see chapter 0). The motivation of taking glass particles instead of biomass ashes was the well-defined chemical composition and particle size range, which helps to reduce uncertainties regarding the interpretation of the results. Moreover, glass particles have a similar composition to silica rich ashes (Table 4). In contrast to the experimental setup of Srinivasachar et al. (1990) and Richter (2003), ECN uses a cooled deposit probe (600°C).

A CFD based sensitivity analysis was performed in order to verify if the stickiness model is able to predict the deposition behavior of the particles. The results of this investigation served as a basis for the subsequent discussion of deviations between the measurement results and the model predictions.

4.1 Experimental setup

Since the glass particle experiments were carried out by ECN and the investigations in this work focus on the modeling part, the experimental setup is only briefly described. The ECN Lab-scale Combustion Simulator (LCS), depicted in Figure 8, is a flexible facility for the characterization of solid fuel combustion and ash deposition behavior. Although the top part of the facility is thermally insulated, a decrease of the mean gas temperature in the direction of the gas flow was observed. In order to quantify this effect, the temperature of the gas was measured along the axis of the reactor tube before the particles were injected. Initially, the particles were introduced into the reactor inlet without a deposit probe. A stainless steel wire mesh, placed inside the reactor and covering its whole cross section was used in order to verify the homogeneity of the particle distribution inside the reactor tube. The cylindrical deposit probe was horizontally arranged in the bottom part of the facility, and the surface temperature of the probe was constant at 600°C. Three test runs were performed, each with constant gas velocities and constant particle diameters as well as varying gas temperatures. The relevant operating data of these test runs are listed in Table 5.

Table 4: Chemical compositions of glass particles used in experimental deposit probe measurements performed by ECN

source		SiO_2	Al_2O_3	FeO	CaO	MgO	Na_2O	K_2O	TiO
ECN	[wt%]	72.3	1.0	-	8.0	4.0	14.2	0.5	-

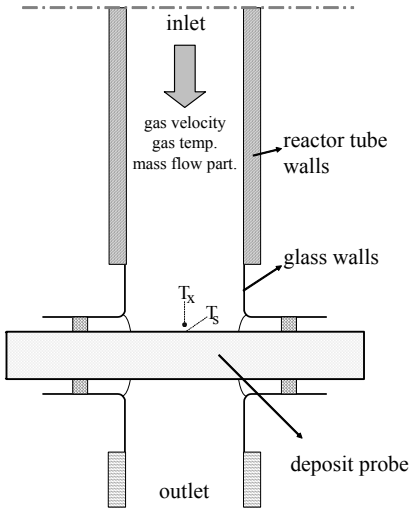

Figure 10: Scheme of the lower part of the lab-scale combustion simulator (LCS) of ECN

Table 5: Operating data of glass particle experiments

test series		case 1	case 2	case3
d_p	[µm]	71	105	105
v	[m/s]	3.1	3.1	6.2
T1	°C	915	870	925
T2	°C	965	940	1005
T3	°C	990	965	1040
T4	°C	1015	1015	1090

T_S = 600°C

Gas composition:
CO_2, H_2O and N_2 mixture

4.2 Comparisons of experimental data with theoretical correlations

Figure 11 shows data measured by ECN, Richter (2003) and Srinivasachar et al. (1990), with the reference viscosity μ_{ref} being plotted as a function of the kinetic energy. A comparison of these data indicates the same tendency of decreasing reference viscosities with increasing kinetic energies. However, the results of ECN do not agree with the derived expression for the reference viscosity.

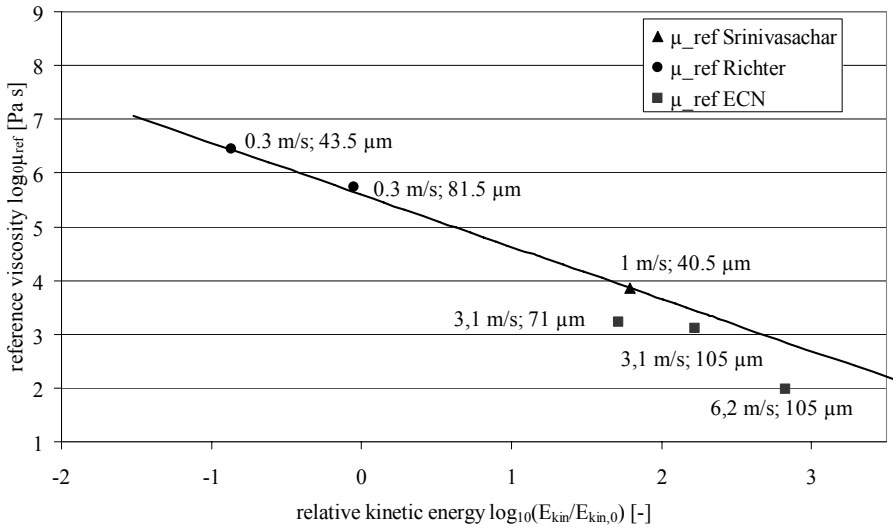

Figure 11: Measured reference viscosities μ_{ref} as a function of relative kinetic energy

Figure 12 shows measured and calculated capture efficiencies of glass particles as a function of gas temperature for three different test runs. The results of the test runs are shown in Table 6. As an example, Figure 13 shows the precipitated glass particles for a capture efficiency of 0.97. At low temperatures no glass particles were found on the surface of the deposit probe, whereas first particle accretions were observed with increasing temperatures. Although the experimental and theoretical data for case 2 are nearly in agreement, the other cases show strong deviations. These deviations were assumed to be caused by erosion, additional adhesion forces, temperature and velocity variations of the gas flow which are not considered in the theoretical calculations as well as other effects. Therefore, detailed CFD analyses of the particle-laden flow in the lab-scale reactor and a discussion of the deviations were conducted.

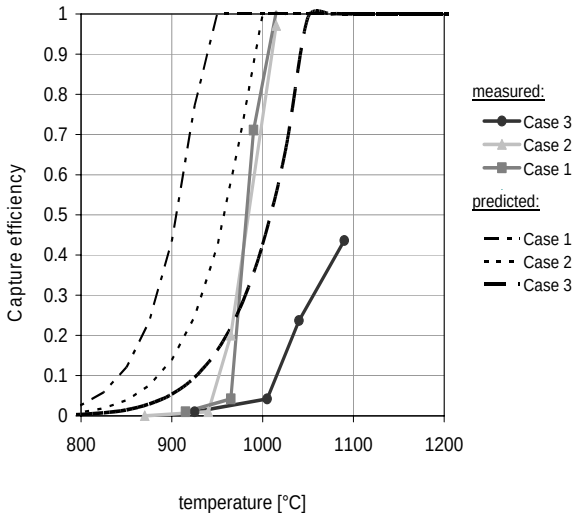

Figure 12: Measured and calculated capture efficiencies for 3 different test runs as a function of gas temperatures

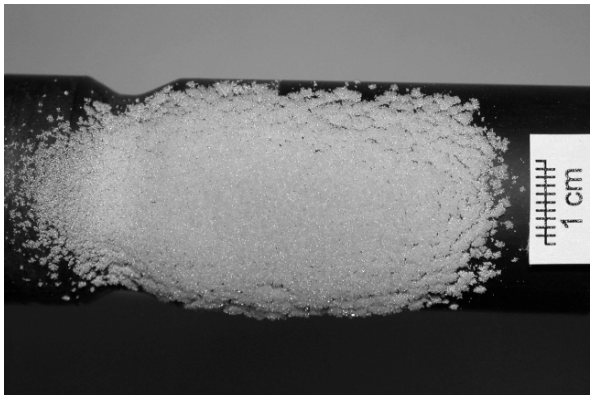

Figure 13: Picture of precipitated glass particles on the deposit probe (d_p = 71 μm, v_p = 3.1 m/s, T = 10°C)

Table 6: Boundary conditions, reference temperatures and reference viscosities determined during deposit formation experiments with glass particles

	diameter	velocity	T_{ref}	μ_{ref}
test cases	[µm]	[m/s]	[°C]	[Pa s]
case 1	71	3.1	1010	$10^{3.2}$
case 2	110	3.1	1020	$10^{3.1}$
case 3	110	6.2	1190	$10^{2.0}$

4.3 CFD analysis of the deposition experiments

CFD simulations were carried out in order to get more detailed information about the underlying processes of particle deposition. These simulations served to calculate the local capture efficiencies of glass particles taking into account local effects on the deposit probe like impaction velocity and impaction angles.

Figure 14 shows the gas velocity profiles in the symmetry plane of the reactor, which strongly vary along the axis of the probe. Consequently, the axis velocity in front of the deposit probe is approximately 23% higher than the bulk flow velocity, whereas the velocities near the wall are significantly lower. The second deviation to the simplified assumption of Equation 3 is related to the temperature field. Due to insufficient insulation of the reactor, the heat loss via the reactor walls must be considered, too. As shown in Figure 14, the gas temperature strongly decreases near the wall.

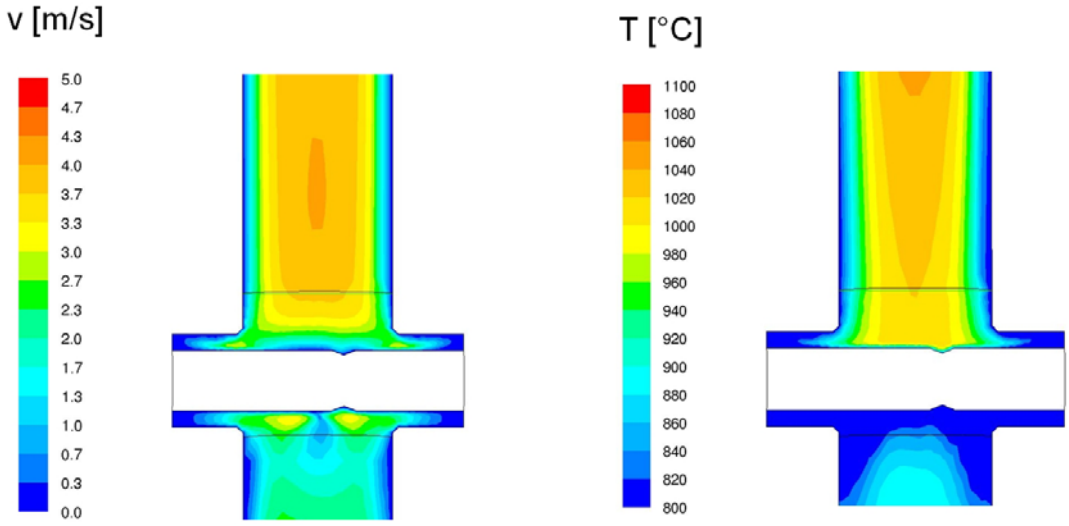

Figure 14: Velocity and temperature profiles in the symmetry plane of the reactor tube (case 2, T=1015°C)

The next step was to analyze the calculated impaction rates of particles on the deposit probe. This was done by comparing CFD simulated impaction rates with calculated impaction rates using a Stokes correlation (Wessel et al., 1988). The Stokes correlation allows the impaction rate on a cylinder to be calculated as a function of particle velocity, particle diameter and diameter of the cylinder (for given particle and gas properties). Since this correlation is based on a homogeneous velocity field around the cylinder, the influence of the velocity distribution was investigated. Figure 15 shows that the calculated (using Stokes correlation) and simulated (using CFD) impaction efficiencies are in agreement. This leads to the conclusion that the velocity distribution due to boundary layer effects of the reactor wall (see Figure 14) had no significant influence on the impaction rates.

Figure 16 shows the distribution of the absolute particle impaction velocity on the deposit probe surface for case 2 of the ECN experiments. While the bulk flow velocity of the gas is 3.1 m/s, the standard deviation of the particle velocities is 0.8 m/s due to the gas velocity gradients in the reactor. The deviations of the particle velocities lead to different kinetic energies resulting in different reference viscosities. Consequently, the temperature at which particles become sticky decreases for particles with lower velocities than the averaged particle velocity (due to an increased reference viscosity as a function of the kinetic energy of the particle), whereas the temperature at which particles are 100% sticky increases for particles that have a higher velocity than the averaged particle velocity. These effects expand the temperature range between non-sticky and fully sticky particles, which reduces the gradient of the capture efficiency as a function of temperature.

In a second step, the superimposed effect of the variation of the temperature of impacting particles on the deposit probe was determined, which has an influence on the viscosity of the particles and therefore on the calculated sticking probability. In each case, the averaged particle temperature was lower than the measured gas temperature T_X (see Figure 10) due to insufficient insulation of the walls and the capture efficiency was shifted

toward higher temperatures. Therefore, the numerical investigations lead to the conclusion that the steep gradient of the measured capture efficiency as a function of the temperature (see Figure 17) cannot be caused by the inhomogeneities of the temperature and velocity fields.

Finally, the influence of the choice of the velocity component for the definition of the kinetic energy of the impacting particle was investigated. The application of the absolute velocity can be justified by the fact that a sticking particle must dissipate the entire kinetic energy. On the other hand, the tangential velocity component could result in a rolling motion of the particle. In Figure 17 the results for both simulation cases are illustrated and compared with experiments. The differences between the two simulations are very small compared to the deviations from the experiments and, therefore, can be neglected.

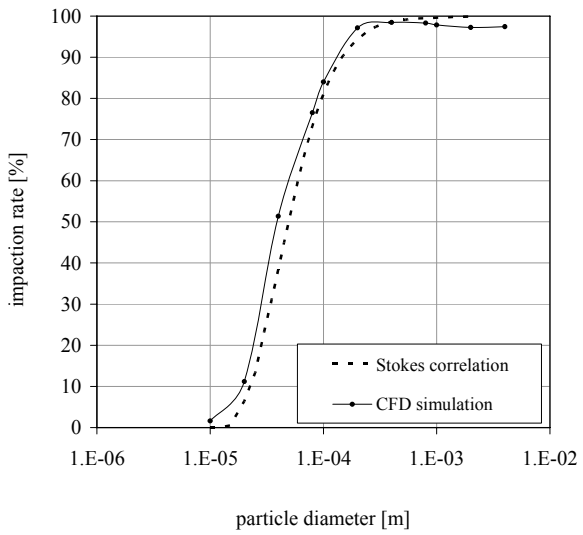

Figure 15: Impaction rates of particles (v_p = 3.1 m/s) – Comparison of the CFD simulation with Stokes correlation (Wessel et al. 1990)

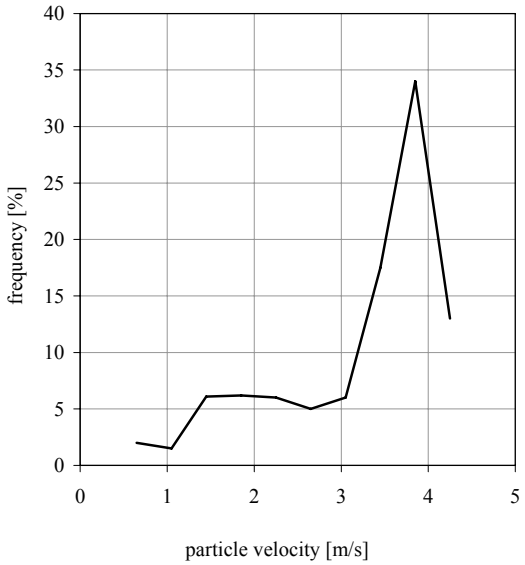

Figure 16: Distribution of the absolute particle impaction velocity on the deposit probe surface

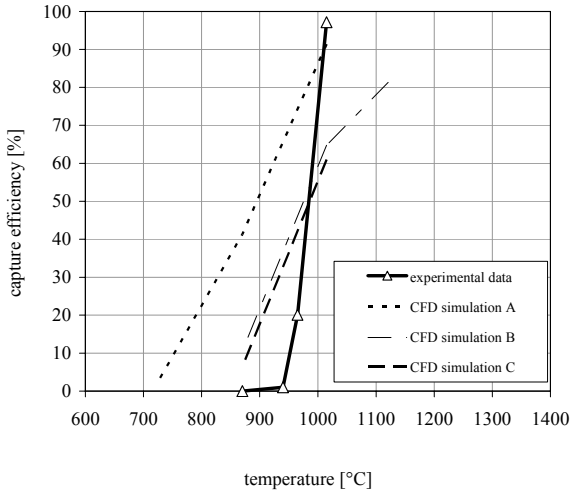

Figure 17: Measured capture efficiencies in comparison with CFD-simulated capture efficiencies (simulation A was carried out using a constant temperature field, simulation B taking the normal component for kinetic energy calculation into account and simulation C using the absolute velocity)

Figure 18 shows the capture efficiencies for different reference viscosities in comparison with experimental data. The diagram indicates that, irrespective of the chosen reference viscosity, the steep increase of the capture efficiency at approximately 975 °C cannot be described by the stickiness approach according to Equation 3. Since the description of the viscosity of glass as a function of temperature is well known, it can be excluded as a possible source for this deviation. Therefore, the only possible reason for the deviations is either the insufficient

description of the capture efficiency by the chosen stickiness approach according to Equation 3 or a potential interaction with other unconsidered effects, which are discussed in the following.

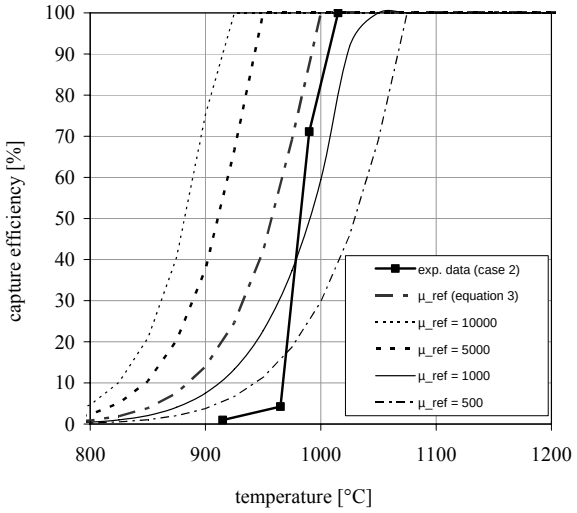

Figure 18: Capture efficiency for different reference viscosities in comparison with experimental data (case 2)

Van Beek (2001) assumed that electric charges caused by the particle impact or atmospheric friction have to be considered in order to predict the capture efficiencies of glass particles. This effect was also identified by the workgroup of Poppe et al. (2000), which investigated the capture efficiencies of glass particles in a range of 2 µm under atmospheric conditions. Although the experimental investigations by Van Beek (2001) and Poppe et al. (2000) were performed under atmospheric conditions, it is assumed that this effect could be important at higher temperatures as well. Furthermore, although the size of the particles investigated in this work is an order of magnitude larger and the considered temperature range is also higher, the influence of electrical charges and the particle deposition behavior might be relevant. Therefore, the importance of this influence should be investigated in further experiments, e.g. by ground fault of the deposit probes used.

Furthermore, the influence of erosion on the deposit layer growth cannot be estimated from the experimental data provided by Srinivasachar et al. (1990), Richter (2003) and ECN. It is assumed that both deposit growth and erosion occur simultaneously. In order to separate the two processes, the experimental setup should be modified. This could be achieved for example by single particle experiments. After a sufficient number of tries with single particles, capture efficiencies can be determined as well. Moreover, the influence of erosion will be modeled separately. This model has to consider both erosion effects due to shear forces of the continuous gas phase and due to particle impaction.

Next, the validity range of viscosities according to Equation 3 has to be taken into consideration. According to Richter (2003), the influence of the surface tension can be neglected for particle viscosities of 10^4 - 10^8 Pas. At higher temperatures, the viscosity can fall below 10^3 Pas, which is also the case for the experiments discussed. Therefore, the influence of the surface tension should be considered as well and additional material properties have to be taken into account.

According to Van Beek (2001), who derived a theoretical approach for capture efficiencies of particles in an atmospheric environment (high particle viscosities), the capture efficiencies depend on additional material properties originating from structural mechanics equations (e.g. Poisson constant and Young´s modulus). Because there is no direct coupling between the viscosity and these additional properties, the model of Walsh (Equation 3) is not appropriate to cover the dependencies in that viscosity range, which becomes generally important for particles with a high viscosity level (e.g. SiO_2 or $3CaO\text{-}2SiO_2$) and particle precipitation in tube bundle heat exchangers of biomass combustion plants. Consequently, a suitable extension of the model must be derived in order consider these influencing parameters.

5 Conclusions

In order to minimize problems related to ash deposit formation in biomass combustion plants, a CFD model for the prediction of deposit formation is being developed as a flexible engineering tool for plant design. At the current state of model development, the effects of condensation of ash forming vapors and precipitation of silica rich coarse fly ash particles in the furnace and the radiative section of the boiler are considered. Mechanisms like the formation and deposition of aerosols as well as erosion have not yet been included in the model.

In order to verify the deposit model and to investigate the sensitivity of the simulation results to the model parameters, simulations were performed for a pilot-scale biomass grate furnace with a fire tube boiler. The simulation results for deposit formation were confirmed by on-site observations. Furthermore, it was found that the deposition of coarse fly ash particles is a dominant effect in deposit formation. Therefore, the quality of the model for this process is the most important factor concerning the prediction accuracy of deposit formation in the plant. Moreover, the simulations showed that the prediction of the fly ash deposition rate is very sensitive to the reference viscosity, which is a model parameter of the viscosity approach applied for silica rich particles. A variation of the reference viscosity within the range of values found in the literature resulted in a change of the total ash deposition rate by a factor of two. However, the simulations showed no significant qualitative difference concerning the distribution of the local deposition rates. In order to achieve a quantitatively improved prediction of ash deposit formation, a new correlation was derived for the reference viscosity as a function of the kinetic energy. Literature data on deposit probe measurements using glass particles as synthetic ash formed the data base for this function. By using this correlation in the simulation of the pilot-scale plant, the range of reference viscosities was determined to be between 30 Pa s and 10^4 Pa s.

Since this was below the range of data found in the literature (10^4 to 10^8 Pa s), deposit probe experiments with glass particles were carried out by ECN, in order to check the validity of the derived correlation for lower reference viscosities, which are typical of biomass combustion plants and boilers. Moreover, the application of the viscosity approach as a stickiness model for silica rich ash particles should be tested and evaluated for such plants.

The comparison of model predictions with ECN's experimental results showed significant deviations in the capture efficiencies. Therefore, a comprehensive analysis was performed in order to investigate possible reasons for these deviations. A CFD analysis of the experiments has led to the conclusion that the broad variation of particle temperatures and velocities due to the experimental setup had no significant influence on the predicted capture efficiencies of the probe and can be excluded as reasons for the deviations. However, electrical charge effects during such experiments as described by other authors could have an influence on the capture efficiency and should therefore be investigated in greater detail and substantially reduced, e.g. by grounding of the deposit probe.

Additionally, the reduction of the deposit layer due to erosion must be considered separately from the stickiness model. Since both effects influenced the formation of the deposit layer, experimental setups have to be modified in order to reduce the influence of erosion. Furthermore, an appropriate erosion model will be implemented in the simulation routines in order to improve the prediction of deposit formation and growth.

Furthermore, it was concluded that additional stickiness sub-models are needed to describe the capture efficiency of particles under the operating conditions of biomass combustion plants. While for lower viscosities $\mu_{part} < 10^4$ Pa s the influence of surface tensions has to be taken into consideration, for high viscosities $\mu_{part} > 10^8$ Pa s the stickiness should be determined based on elastic and plastic deformations of the impacting particles. Furthermore, the independency of the reference viscosity from the ash particle compositions should be verified.

To sum up, an important tool for efficient biomass furnace and boiler design is currently under development. The influence of the fuel and the operating conditions on the deposit formation processes can be investigated as early as the design phase allowing for appropriate measures to be taken in order to reduce deposit formation. Even at the present state of development, the model can assist in plant design by providing initial qualitative information. However, further experimental investigations as well as the development and validation of additional sub-models are necessary in order to improve the prediction accuracy of the model under development. Moreover, the deposit model will be coupled with a CFD model for heat exchanger tube bundles in order to allow an investigation of the deposit formation process in the whole plant including the convective section of the boiler.

Nomenclature

$\dot{N}_{cond}$	Ash vapor condensation flux (mol/m^{2}s)
c_w	Saturation concentration of ash forming vapor at wall (mol/m^3)
c_∞	Concentration of ash forming vapors in free stream (mol/m^3)
d_p	Particle diameter (µm)
E_{kin}	Kinetic energy of impaction particle (J)
$E_{kin,0}$	Kinetic energy of reference particle = 4.35e-11(J)
k	Turbulence kinetic energy (m^2/s^2)
p_{cond}	Sticking probability of condensed deposit layer (-)

p_{part}	Sticking probability of particle (-)
p_{tot}	Total sticking probability of impacting particle (-)
p_{wall}	Sticking probability of wall (-)
v	velocity (m/s)
T	Temperature (°C)

Greek Symbols

β	Condensation coefficient (m/s)
ε	dissipation rate (m^3/s^2)
μ_{part}	Viscosity of particle (Pa s)
μ_{ref}	Reference viscosity (Pa s)

Abbreviations

CFD	Computational Fluid Dynamics
ISAT	In-Situ Adaptive Tabulation algorithm
LCS	Lab-scale Combustion Simulator

Acknowledgements

The work presented was supported by the Kplus program of the Austrian Bioenergy Centre GmbH. Moreover, the deposit probe measurements were performed by ECN Energy research Centre of the Netherlands, Unit Biomass, Coal and Environmental Research, which was supported by the EU within the project "BIOASH" (SES6-CT-2003-502679).

References

Backman, R., Hupa, M., Skrifvars, B-J., 1997. Predicting superheater deposit formation in boilers burning biomass, Proceedings of the conference on impact of mineral impurities in solid fuel combustion, 405-416.

Baehr, H.D., Stephan, K., 1996. Wärme- und Stoffübertragung, 2nd edition, Springer, Berlin.

Baxter, L.L., Miles, T.R., Miles Jr., T.R., Jenkins, B.M., Milne, T., Dayton, D., Bryers, R.W., Oden, L.L., 1998. The behaviour of inorganic material in biomass-fired power boilers: field and laboratory experiences, Fuel Processing Technology 54, 47-78.

Forstner, M., Hofmeister, G., Jöller, M., Dahl, J., Braun, M., Kleditzsch, S., Scharler, R., Obernberger, I., 2006. CFD simulation of ash deposit formation in fixed bed biomass furnaces and boilers, Progress in Computational Fluid Dynamics, Vol. 6, Nos. 4/5, 248-261.

Frandsen, F., Hansen, J., Jensen, P.A., Dam-Johansen, K., Hørlyck, S., Karlsson, A., 2003. Ash and deposit formation in the biomass co-fired Masnedø combined heat and power production plant, IFRF Combustion Journal, article number 200304.

Jensen, P.A., Stenholm, M., Hald, P., 1997. Deposition investigation in straw-fired boilers, Energy & Fuels, 11, 1048-1055.

Kær, S.K., 2001. Numerical investigation of ash deposition in straw-fired boilers, Ph.D. thesis, Aalborg University, Aalborg, Denmark.

Kær, S.K., 2004. Numerical modelling of a straw-fired grate boiler, Fuel, Vol. 83, 1183-1190.

Lee, F.C.C., Lockwood, F.C., 1999. Modelling ash deposition in pulverised coal-fired applications, Progress in Energy and Combustion Science, 25, 117-132.

Mueller, C., Skrifvars, B.J., Backman, R., Hupa, M., 2003. Ash deposition prediction in biomass fired fluidised bed boilers – combination of CFD and advanced fuel analysis, Progress in Computational Fluid Dynamics, 3, 112-120.

Poppe T., Blum J., Henning Th., 2000. Analogous Experiments on the Stickiness of Micron-Sized Preplanetary Dust, Astrophys. J., 533, 454-471.

Richards, G.H., Slater, P.N., Harb, J.N., 1993. Simulation of ash deposit growth in a pulverized coal-fired pilot scale reactor, Energy & Fuels 7, 774-781.

Richter, S., 2003. Numerische Simulation der Flugaschedeposition in kohlestaubgefeuerten Dampferzeugern, Fortschritt-Berichte VDI, Reihe 6, Nr. 501, VDI Verlag, Düsseldorf, Deutschland.

Scharler, R., 2001. Entwicklung und Optimierung von Biomasse-Rostfeuerungen durch CFD-Analyse, Ph.D. thesis, Graz University of Technology, Graz, Austria.

Scharler R., Obernberger I., 2002. Deriving guidelines for the design of biomass grate furnaces with CFD analysis – a new Multifuel-Low-NOx furnace as example, in: Proc. of the 6th European Conference on Industrial Furnaces and Boilers, Estoril, Portugal, Editors: INFUB, Rio Tinto, Portugal.

Scharler R., Forstner M., Braun M., Brunner T., Obernberger I., 2004. Advanced CFD analysis of large fixed bed biomass boilers with special focus on the convective section, in: Proc. of the 2nd World Conference and Exhibition on Biomass for Energy, Industry and Climate Protection; Editors: ETA-Florence, Rome, Italy, Vol. II, 1384-1387.

Senior, C.L., Srinivasachar, S., 1995. Viscosity of Ash Particles in Combustion Systems for Prediction of Particle Sticking, Energy & Fuels 9, 277-283.

Srinivasachar, S., Helble, J.J., Boni, A.A., 1990. An Experimental Study of the Inertial Deposition of Ash under Coal Combustion Conditions, 23rd Symposium on Combustion, The Combustion Institute, 1305-1312.

Urbain, G., Cambier, F., Deletter, M., Anseau, M.R., 1981. Viscosity of silicate melts, Transactions and Journal of the British Ceramic Society 80, 139-141.

Van Beek, M.C., 2001. Gas-side fouling in heat-recovery boilers, Ph.D. Thesis, Eindhoven University of Technology, The Netherlands.

Walsh, P.M., Sayre, A.N., Loehden, D.O., Monroe, L.S., Beer, J.M., Sarofim, A.F., 1990. Deposition of bituminous coal ash on an isolated heat exchanger tube: effects of coal properties on deposit growth, Progress in Energy Combustion Science 16, 327-346.

Wessel, R.A., Righi, J. 1988. Generalized Correlations for Interial Impaction of Particles on a Circular Cylinder, Aerosol Science and Technology, Vol 9, 29-60.